Pharm Res (2012) 29:1319–1327
DOI 10.1007/s11095-012-0710-z

RESEARCH PAPER

Controlled Cell Death by Magnetic Hyperthermia: Effects of Exposure Time, Field Amplitude, and Nanoparticle Concentration

L. Asín • M. R. Ibarra • A. Tres • G. F. Goya

Received: 30 August 2011 / Accepted: 15 February 2012 / Published online: 24 February 2012

ABSTRACT

Purpose To investigate the effects of alternating magnetic fields (AMF) on the death rate of dendritic cells (DCs) loaded with magnetic nanoparticles (MNPs) as heating agents. AMF exposure time and amplitude as well as the MNPs concentration were screened to assess the best conditions for a controlled field-induced cell death.

Methods *Human-monocyte-derived* DCs were co-incubated with dextran-coated MNPs. The cells were exposed to AMF (f=260 kHz; $0 < H_0 < 12.7$ kA/m) for intervals from 5 to 15 min. Morphology changes were assessed by scanning electron microscopy. Cell viability was measured by Trypan blue and fluorescence-activated cell sorting (FACS) using Annexin-propidium iodide markers.

Results We were able to control the DCs viability by a proper choice AMF amplitude and exposure time, depending on the amount of MNPs uploaded. About 20% of cells showed Annexin-negative/PI-positive staining after 5–10 min of AMF exposure.

Conclusions Controlled cell death of MNP-loaded DCs can be obtained by adequate tuning of the physical AMF parameters and MNPs concentration. Necrotic-like populations were observed after exposure times as short as 10 min, suggesting a fast underlying mechanism for cell death. Power absorption by the MNPs might locally disrupt endosomic membranes, thus provoking irreversible cell damage.

KEY WORDS alternating magnetic fields · cell death · dendritic cells · magnetic hyperthermia · magnetic nanoparticles

INTRODUCTION

Within the context of clinical multimodal therapies hyperthermia is an adjuvant therapy for cancer treatment, whose first applications can be traced back to the beginning of the 20th century (1,2). The synergistic effect of hyperthermia at 42–43°C when combined with radiotherapy is well established at human clinic, and also its enhancing effects with numerous cytotoxic drugs such as taxane, paclitaxel, or docetaxel have been reported (3). Hyperthermia using a combination of alternating magnetic fields (AMF) and magnetic microparticles as heating agents was first reported along the 80's (4), but was in 1993 when the first prospective study for clinical applications in humans was reported (5). In 2010, magnetic hyperthermia trials based on the use of MNPs have passed preclinical stages and received regulatory approval as a new clinical therapy named thermotherapy (6).

Although important advances regarding early tumor detection have been accomplished (7), a good number of the

Electronic supplementary material The online version of this article (doi:10.1007/s11095-012-0710-z) contains supplementary material, which is available to authorized users.

L. Asín • M. R. Ibarra • G. F. Goya
Instituto de Nanociencia de Aragón (INA), University of Zaragoza
Mariano Esquillor s/n
50018 Zaragoza, Spain

M. R. Ibarra • G. F. Goya
Departamento de Física de la Materia Condensada
Facultad de Ciencias, Universidad de Zaragoza
Zaragoza, Aragon 50009 Spain

A. Tres
Oncology Department, Hospital Universitario "Lozano Blesa"
50009 Zaragoza, Spain

G. F. Goya (✉)
Instituto de Nanociencia de Aragón
Mariano Esquillor s/n, Campus Rio Ebro
Zaragoza 50018 Spain
e-mail: goya@unizar.es

cancer cases are diagnosed when the disease is in advanced stage, and therefore early detection remains among the biggest challenges in oncology. The use of MNPs as heating agents would result in a more selective elimination of targeted cells, but a major obstacle for this approach is the rethiculoendothelial system (RES) that detects and phagocytes MNPs, preventing targeting and therapeutic action (8). An alternative strategy for targeting neoplasic tissues is to magnetically charge system cells *ex vivo*, in order to evade the RES. Recent experiments *in vitro* using magnetically-loaded dendritic cells (DCs) as vectors for thermotherapy have shown the potential of this 'Trojan horse' strategy for immune-related therapies (9).

DCs constitute an active part of the immune system, performing (among other) vigilant functions and triggering the immune response mediated by T cells (10). The main hallmark of DCs is that they are specialized in capturing and processing antigens (11,12). Due to this fact, DCs are considered as the most important antigen presenting cells (APCs). The ability of the DCs to potently activate T cells depends on some specific features of their mature state, such as high expression of MHC I, MHC II and co-stimulatory molecules. Moreover, the migration capability of DCs to lymph nodes is essential to activate those T cells that recognize the antigens (13).

It has been reported that DCs are able to incorporate not only antigens, but also inorganic particles (14). This ability to incorporate several kinds of antigens and/or particles makes these cells excellent candidates for transport, vectorization and delivery of drugs for immune-related therapies. Uptake of antigens by DCs may occur by differentiated processes such as macropynocitosis, phagocytosis or receptor-mediated endocytosis (15) and, more recently, the ability of DCs to incorporate several kinds of solid particles within a broad size range has also been described (16).

In this work we present and discuss a series of *in vitro* experiments using DCs as immuno-compatible vehicles of MNPs. The lack of a systematic study of cell death using magnetic hyperthermia has been the motivation of the present work, which focuses on experiments designed to induce cell death by applying an AMF on MNP-loaded DCs in a controlled way. The amplitude of the magnetic field, application time and magnetic upload of the DCs were varied to assess the conditions that trigger the cellular death, aiming to find the appropriate parameter window for potential therapeutic protocols.

MATERIALS AND METHODS

Magnetic Nanoparticles

Commercially available MNPs used in this work were composed of a magnetite core (Fe_3O_4) with a carboxyl-functionalized dextran shell at the surface (*nanomag®-D, Micromod GmbH, Germany*) (17). From Transmission Electron Microscopy (TEM) and Dynamic Light Scattering (DLS) we found an average core size of $<d>=15(2)$ nm and hydrodynamic diameter $d_H=217(2)$ nm in dH_2O. Also the specific power absorption of these MNPs (i.e., their efficiency as heating agents) has been measured by AMF application under the same experimental conditions used for the *in vitro* experiments on DCs (see below). The main parameters are displayed in Table I. Detailed structural and magnetic characterization of these MNPs can be found elsewhere. (9)

Dendritic Cell Differentiation from PBMCs

Peripheral blood mononuclear cells (PBMCs) were isolated from normal blood by density gradient (*Ficoll Histopaque-1077, Sigma*). Cells were washed twice with PBS at 1200 rpm and then centrifuged 10 min at 800 rpm to avoid platelet contamination. Isolation of CD14+ cells was performed with magnetic beads (*CD14 Microbeads, Miltenyi*) by positive immunoselection using the autoMACS Separator (Miltenyi). Positive CD14+ cells (10^6 cells/ml) were cultured in RPMI 1640 (*Sigma*) with 10% FBS, 1% glutamine, 1% antibiotics and supplemented with IL-4 (25 ng/ml) and GM-CSF (25 ng/ml)(*Bionova*), for 5 days at 37°C. Every second day, medium was replaced by fresh medium containing the same concentration of interleukins. DCs phenotype was characterized by flow cytometry as described elsewhere (9).

DCs Culture for *In Vitro* AMF Experiments and Quantification of MNPs

For *in vitro* magnetic hyperthermia experiments, DCs cultured as described above were collected and seeded into a 24-wells plate at 10^6 cells/ml. NPs suspension was added at concentrations of 50 pg(Fe_3O_4)/cell and 20 pg(Fe_3O_4)/cell (corresponding to 36.18 and 14.47 pg(Fe)/cell, respectively) in two wells each. Two additional wells, each containing 10^6 cells/ml without MNPs, were used as a control. Cells were incubated overnight at 37°C. Next day, cells were collected from each well and washed four times with fresh medium to remove the non incorporated NPs. Cells were counted and re-suspended in 500 µl of complete medium. Extensive research studies of cytotoxicity effect of MNPs in DCs were performed and reported elsewhere (9). Briefly, no cytotoxic effects were found in DCs after up to 5 days of incubation in presence of 50 pg(Fe_3O_4)/cell (36.18 pg(Fe)/cell).

In order to quantify the amount of uploaded MNPs per cell, magnetization measurements were performed in a SQUID (Superconducting Quantum Interference Device) magnetometer (MPMS-XL, Quantum Design). The magnetic characterisation of colloids and cell cultures was made

Table 1 Physicochemical Properties of the MNPs Functionalized With Carboxyl Surface Groups: Core Size (d_{CORE}); Hydrodynamic Size (d_H); Size Distribution (σ_H); Saturation Magnetization (M_S), Coercive Fields H_C and Specific Power Absorption (SPA)

Sample	Core material	Surface charge	d_{CORE} (nm)	d_H (nm)	σ_H	M_S (emu/gFe_3O_4)	H_C (Oe)	SPA (W/g)
COOH(MNP)-	Fe_3O_4	$COOH^-$	15(2)	217(2)	0.43	68.0	12(5)	46(6)

through static measurements as a function of field at different temperatures. Both samples were measured *as is* (i.e., in the liquid phase) after being conditioned in sealed sample holders with 200-μL capacity. Magnetisation data were collected in applied magnetic fields up to 4 MA/m at temperatures of 5 K and 250 K to avoid the melting of the frozen liquid carrier. The average amount of MNPs internalized per cell was obtained from the M(H) curves of the samples, by comparing the saturation magnetization (M_S) of the cells with that of the MNPs in the pure colloid with known concentration.

Specific Power Absorption Experiments

The specific power absorption (SPA) of the pure magnetic colloids (concentration 10 mg(Fe_3O_4)/ml) was measured with a commercial ac field applicator (DM100 by nB nanoscale Biomagnetics, Spain) working at f=260 kHz and field amplitudes H_0 from 0 to 12.7 kA/m. Experiment were carried within a thermally-insulated working space of about 1 cm^3, using a closed container of 0.5 ml volume conditioned for measurements in liquid phase.

Each series of AMF experiments on cultured DCs were designed as a '2×2' setup (see Fig. 1). In these kind of experiments, two pairs of samples were organized as follows: the first pair of samples consisting of *as cultured* blank DCs (i.e., without nanoparticles, Fig. 1a) and NP-loaded DCs (Fig. 1b), were not exposed to magnetic fields and analyzed at the end of the experiment in order to compare the natural viability of the cell culture.

The second pair of samples, blank and NP-loaded DCs (Fig. 1c and d, respectively), were exposed to the alternating magnetic field while measuring the medium temperature with an optic fiber thermometer placed inside the sample holder. All the experiments reported in this work were performed in this 2×2 procedure, at the selected AMF frequency of f=260 kHz. In order to study the conditions for cell death triggering, different AMF amplitudes (H_0= 3.2, 6.4, 9.5 and 12.7 kA/m), and application times (5, 10 and 15 min) were chosen. All experiments were done at least in triplicate.

After the field exposure, cell viability was measured in the four samples, using trypan blue and FACS by annexin-propidium iodide (PI) staining. The trypan blue assay was conducted by diluting 10 μl of cell samples into 0.4% trypan blue solution (1:1). Cells were counted in an optical microscopy and differentiating those that were stained in blue (death cells) and those unstained (living cells). DCs viability was also tested by flow cytometry using a commercial kit (Immunostep, Spain). DCs (10^6) of each sample were re-suspended in Annexin-binding buffer and stained with 5 μl of Annexin and 5 μl of propidium iodide. DCs were incubated for 15 min in darkness at room temperature. Analysis of the results was performed using a FACSAria Cytometer and FACSDiva software.

Cell Morphology by Scanning Electron Microscopy (SEM)

The cell morphology before and after AMF application was analyzed by scanning electron microscopy (SEM) images, obtained with a FEI INSPECT F microscope. The samples were prepared by fixing the cells with 2.5% glutaraldehyde in 0.1 M sodium cacodylate and a 3% sucrose solution for 90 min at 4°C. For dehydration the cells were incubated for 5 min with increasing concentrations of methanol. Before SEM observation all samples were sputter-coated with gold.

RESULTS

The effects of AMF on magnetically-loaded DCs and the corresponding control samples in the 2x2 experiment are shown in Fig. 2. These results were obtained by applying an AMF during an application time t_{app}=30 min (f=250 kHz, H_0=12.7 kA/m) on DCs incubated with a concentration C_{NP}=50 pg(Fe_3O_4)/cell (36.18 pg(Fe)/cell), as previously reported (9). It is clear that a major percentage (95±4%) of death is only achieved for the magnetically-loaded DCs, whereas those cells not loaded with MNPs were not affected by the AMF application during the same time interval. Furthermore, we found that reducing the application times to 15 minutes yielded very similar values of cell death (see below). Thus, these experimental parameters were considered as the upper limit for the energy needed to be delivered during experiments and, in order to find the conditions for a controlled cell death, we further explored different combinations of field amplitudes H_0, nanoparticles concentrations C_{NP}, and application times (t_{app}).

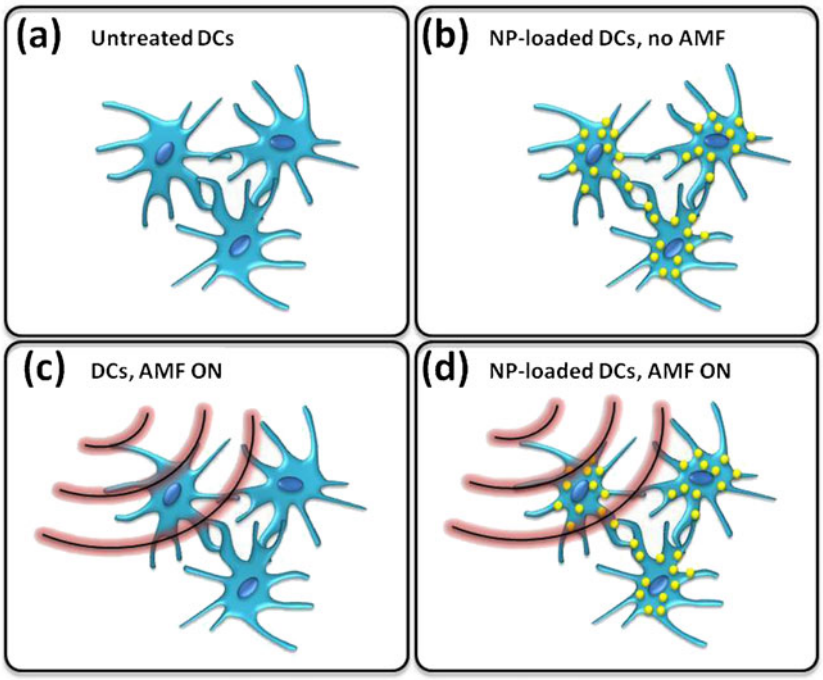

Fig. 1 Illustration for the design of the '2 × 2' experiment: (**a**) Untretated DCs. (**b**) DCs loaded with MNPs, no AMF application, (**c**) DCs exposed to AMF, and (**d**) DCs loaded with MNPs and exposed to AMF.

The SEM images revealed (see Fig. 3) that the observed cell death after AMF application toMNP-loaded DCs is accompanied by the concurrent loss of the complex structure of the cell membrane that is typical of this kind of cells. It can also be noticed in Fig. 3b the appearance of membrane channels as a consequence of AMF application, which is likely the responsible mechanism to turn the membrane permeable.

Figure 4 shows the experimental results of a series of AMF application experiments using different field amplitudes H_0 (with f=260 kHz, t_{app}=15 min), together with the three controls (CDs: CDs without MNPs and no AMF; CDs + AMF: CDs without MNPs and AMF application at H_0=12.7 kA/m;

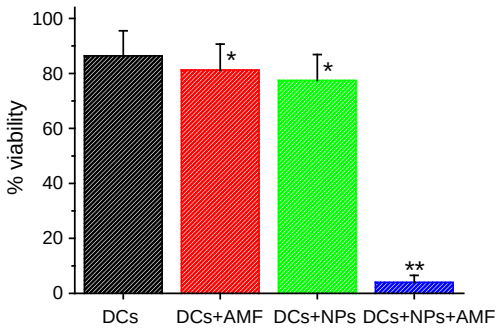

Fig. 2 DC viability results (n=6) for the 2 × 2 experiment illustrated in Fig. 1. DCs: control DCs samples; DCs + AMF: DCs without MNPs after 30 min of AMF; DCs + NPs: DCs with 50 pg(Fe_3O_4)/cell (36.18 pg(Fe)/cell) and without AMF, and DCs + NPs + AMF: DCs with 50 pg(Fe_3O_4)/cell after applying AMF (H_0=12.7 kA/m, f=260 kHz, t=30 min). FACS analysis was performed about 3–4 h after AMF exposure. Data represent the mean + SD, n=4. * P < .05 and ** P < 0.0005 as compared with control sample.

and DCs + NPs: DCs incubated with 50 pg(Fe_3O_4)/cell (36.18 pg(Fe)/cell) but without AMF). It can be seen that the effect of increasing the field amplitude from 6.4 to 12.7 kA/m resulted in a decrease of cell viability from 55% to 25%, to be compared with the ≈80–85% of the three control samples. Similar trends were observed for lower concentration of MNPs (20 pg(Fe_3O_4)/cell) used during the incubation with DCs (see Figure S1 of the Supplementary Material).

We have quantified the actual mass of MNPs incorporated by DCs as a function of the concentration added during overnight incubation. For this purpose we used the data from magnetic measurements of the MNP-loaded DCs, normalized to the number of cells (i.e., 10^6 DCs in each well) and a control sample (DCs without MNPs) to account for the diamagnetic signal from the DCs. The results of DCs cultured with increasing concentrations (up to 300 pg(Fe_3O_4)/cell), demonstrated that the amount of MNPs incorporated into DCs increased with an approximate linear dependence for low values of the added concentration (Figure S3 in Supplementary Material). However, for added MNPs concentration larger than 150 pg(Fe_3O_4)/cell a non-linear increase of the magnetic signal was observed, which we attributed to an excess of MNPs remaining in the culture medium the cell cultures based on the brownish colour observed in the cell medium at those highest concentrations. This colouring of the cell medium clearly indicates that the excess of MNPs that were not incorporated by DCs could not be totally removed even after several washing times. It has to be noted, however, that all AMF experiments reported here were conducted at much lower concentrations of MNPs (i.e., 20 and 50 pg

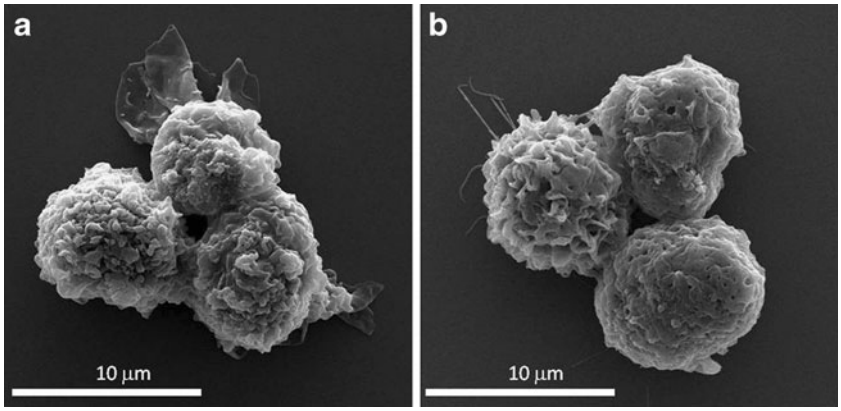

Fig. 3 SEM images of DCs loaded with MNPs (**a**) before and (**b**) after the application of the AMF. A partial collapse of the membrane structures can be observed after exposure to AMF.

(Fe_3O_4)/cell, where the colouring of the medium was not observed) and thus with negligible amounts of MNPs in the medium. Using the M_S values for the pure ferrofluid and the average volume of the magnetic cores extracted from TEM images, the average number of MNPs per cell was determined to be 90 to 1.2×10^3 MNPs/cell (0.40 to 5.30 pgFe/cell). This relatively small number of particles was able to induce cellular death when submitted to an AMF, as will be discussed in the next sections.

Figure 5 shows the effect of increasing the AMF exposure time on cell viability, after overnight incubation with a fixed concentration of MNPs C_{NP}=20 pg(Fe_3O_4)/cell. It can be seen that after 5 minutes of AMF application the cell viability does not significantly decreases. Moreover, both TB and FACS methods give coincident values within experimental error. However, increasing the application time to 10 minutes resulted in a smaller viability of 65% of the total cells as measured by TB technique, whereas FACS analysis showed about 50% of cell viability. After 15 minutes of AMF application the viability further decreased, again showing appreciable differences between the results obtained from TB and FACS techniques.

A similar series of experiments performed using a higher concentration of MNPs during incubation (C_{NP}=50 pg (Fe_3O_4)/cell) resulted in the same gradual increase of cell death with AMF application times, as shown in Fig. 6. At this concentration, only 10 minutes of AMF exposure time was required to reduce the cell viability to less than 50%. In agreement with the larger amount of incubated MNPs used in these experiments, the final percentage of cell viability at each AMF application time was found to be systematically lower when compared to those DCs cultured with C_{NP}=20 pg (Fe_3O_4)/cell (see Fig. 6).

For the 'extreme' conditions of AMF exposure (i.e., H_0= 12.7 kA/m, t_{app}=15 min), a systematic difference was observed in cell viability results as obtained from TB and

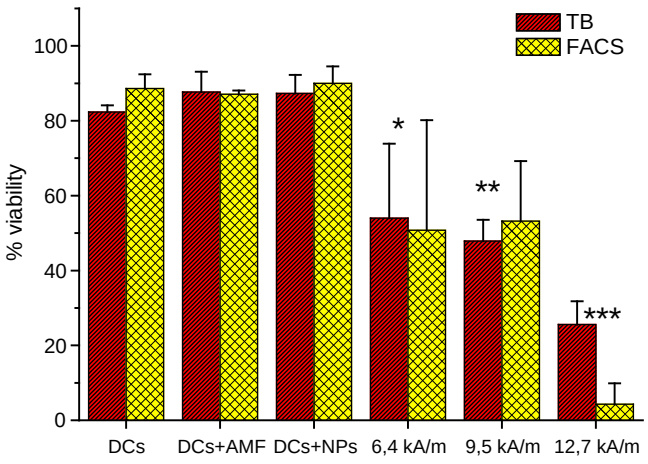

Fig. 4 Effect of the AMF amplitude H_0 (at f=260 kHz, t=15 min) on the cell viability of DCs incubated with 50 pg(Fe_3O_4)/cell (36.18 pg(Fe)/cell), as measured by Trypan Blue and Fluorescence-activated cell sorting (FACS). Viability analysis were performed 15 min and 3–4 h after AMF experiments for TB and FACS, respectively. The H_0 used for the reference sample (DCs + AMF) was 12.7 kA/m. Data represent the mean ± SD, n=2. * $P<0.1$; ** $P<0.05$ and ***$P<0.0025$ as compared with control sample.

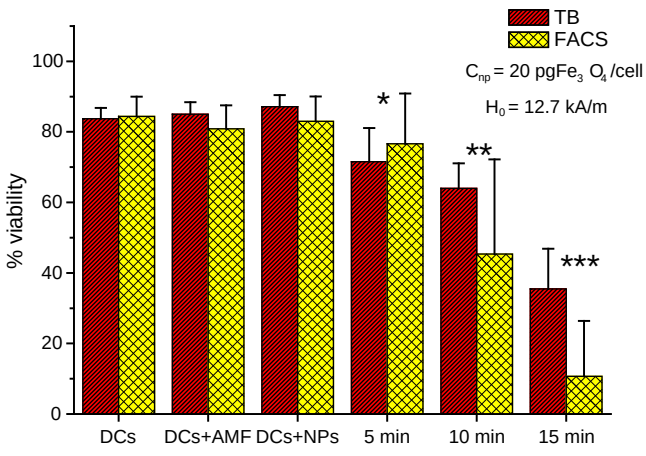

Fig. 5 Effect of different AMF application times t (at f=260 kHz, H_0= 12.7 kA/m) on the cell viability of DCs incubated with 20 pg(Fe_3O_4)/cell (14.47 pg(Fe)/cell), as measured by Trypan Blue and Fluorescence-activated cell sorting (FACS). Viability analysis were performed 15 min and 3–4 h after AMF experiments for TB and FACS, respectively. The time exposure for the reference sample (DCs + AMF) was 15 min. Data represent the mean ± SD, n=4. * $P<0.1$; ** $P<0.025$ and ***$P<$ 0.0005 as compared with control sample.

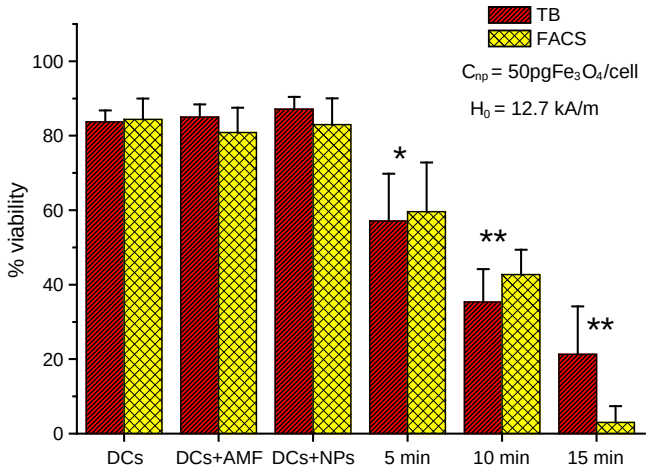

Fig. 6 Effect of different AMF application times t (at f=260 kHz, H_0= 12.7 kA/m) on the cell viability of DCs incubated with 50 pg(Fe_3O_4)/cell (36.18 pg(Fe)/cell), as measured by Trypan Blue (TB) and Fluorescence-activated cell sorting (FACS). Viability analysis were performed 15 min and 3–4 h after AMF experiments for TB and FACS, respectively. The time exposure for the reference sample (DCs + AMF) was 15 min. Data represent the mean ± SD, n=4. * $P<0.01$ and ** $P<0.0005$ as compared with control sample.

FACS protocols on the same samples. For example, it can be seen in Fig. 4 (at H_0=12.7 kA/m) and Fig. 6 (at t_{app}= 15 min) that TB yielded larger fraction of viable cells after AMF exposure. Since the analysis by both protocols were completed after different time intervals (i.e., 15 min and 3–4 h after AMF exposure for TB and FACS, respectively), we performed a specific experiment to analyze the evolution of the DCs viability by TB protocol at different times after the AMF exposure (H_0=12.7 kA/m; f=260 kHz; C_{NP}=50 pg (Fe_3O_4)/cell and t_{app}=15 min). The results (see Fig. 7) showed that immediately after the experiment the amount of viable cells was about 60%, and a small but noticeable decrease (to 52%) when analyzed after 15 min with the same protocol. However, after 4 h the TB analysis revealed a major decrease (to less than 2%) of viable cells in the same sample. These results confirmed that some of the cells

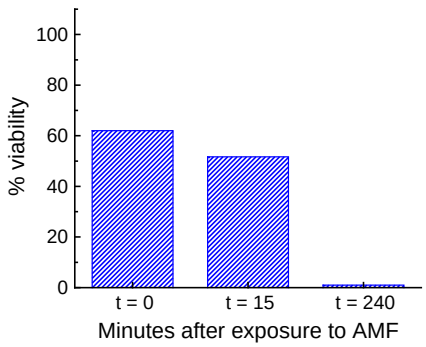

Fig. 7 Viability of magnetically loaded DCs by Trypan Blue at different times after a single AMF application of 15 min. Immediately after AMF application (t=0), 15 min (t=15) and 4 hours (t=240) after the application of AMF. The field parameters were H_0=12.7 kA/m, f=260 kHz.

damaged during the AMF exposure appear as 'healthy' cells within few minutes after, and explain the differences observed between FACS and TB protocols in all the hyperthermia experiments performed.

In order to determine whether the exposure to AMF had any effect on the fraction of viable DCs, we exposed DCs samples to AMF for different times and followed cell viability a) immediately and b) one day after experiment, using FACS measurements. Figure 8 demonstrates that the viability of DCs showed no significant difference after 4 and 28 h after AMF application, indicating that those cells surviving to AMF exposure remain viable, without any long-term effects.

To discriminate apoptotic and necrotic cell death, the cells were stained with Annexin V-FITC and PI, and the resulting DCs distributions obtained from FACS were analyzed. Figure 9 shows typical results obtained at different conditions of AMF amplitude, exposure time and NPs concentrations. About 20 to 50% of the DCs population (depending on experimental conditions) showed Annexin V-negative/PI-positive staining after AMF exposure times as short as 10 min) indicating a necrotic-like process, whereas approximately 9–10% of the cells were Annexin V-positive/PI-negative (identical to control samples within errors). The percentages of the stained cells observed within the four quadrants of FACS results remained essentially constant after 4 and 28 h after AMF experiments.

DISCUSSION

As a general result from these systematic series of experiments, it is clear that the exposure of MNP-loaded DCs to AMF reduced the cell viability in an amplitude- and time-dependent manner. Furthermore, for a given set of AMF parameters, the (average) amount of uploaded MNPs has a clear effect on the final fraction of death cells.

Most of the previous works on magnetic hyperthermia using a wide variety of cell lines have associated the decrease in cell viability to the temperature increase observed during the experiments (18–22). However, it is not clear how the small amount of incorporated magnetic material (of the order of few pg(Fe_3O_4)/cell) can be able to increase the temperature of the whole cell medium to the required 44–46°C for hyperthermia-triggered apoptosis mechanisms (22). In a previous work (23), a theoretical study on the feasibility of rising the intracellular temperature to reach the necessary conditions for hyperthermia has been reported. The author concluded that only for a cluster of several cells fully loaded with MNPs could the conditions for hyperthermia be fulfilled. The theoretical model of ref. (23) also indicated that, for a isolated single cell filled with MNPs, the increase of temperature to hyperthermal conditions was highly improbable. It is important to note that these

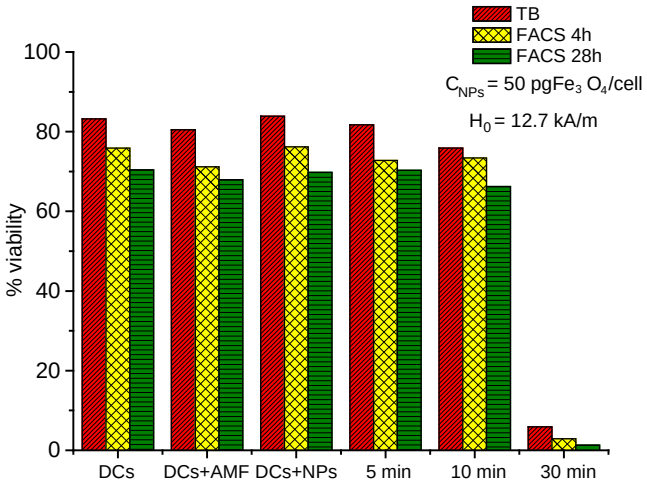

Fig. 8 Viability of magnetically loaded DCs after AMF application (f=260 kHz, H_0=12.7 kA/m) at a NPs concentration of 50 pg(Fe_3O_4)/cell (36.18 pg(Fe)/cell), as measured by TB 15 min after the experiments (*red dashed bars*); FACS measured 3 to 4 h after experiments (*crossed yellow bars*), and FACS 28 h after experiments (*horizontal dashed green bars*). The time exposure for the reference sample (DCs + AMF) was 30 min.

arguments are referred to the impossibility of a *temperature increase* on a single cell, and does not analyze any effect of the power release on biological units such as membranes.

A key issue from the present experiments was that the temperature of the cell cultures remained essentially constant during AMF application. This effect was observed in every single experiment within the values of field amplitude, frequency and MNPs concentration used in this work. The relevance of this result is related to the evidenced ability of the MNPs to produce cellular damage by a different mechanism than the global increase of temperature (i.e., hyperthermia), yielding to cell death. Together, the absence of temperature increase and the data from Figs. 7 and 8 support the hypothesis that the cell damage remotely induced by the AMF operates at the intracellular level. Based on these ideas and the improbable increase of intracellular temperature as argued by Rabin (23), we hypothesized that it is not the temperature but the power released by the MNPs during AMF application that might affect cellular functional units such as proteins or membranes, causing the observed cell death.

It has been recently observed by other groups that the application of AMF on MNP-loaded cells can produce a large decrease in cell viability without actual temperature increase of the cell medium (24,25). Consistently with these results, theoretical calculations from a model of MNPs-membrane interactions suggested that the effects of the power released by MNPs under AMF is to destroy the

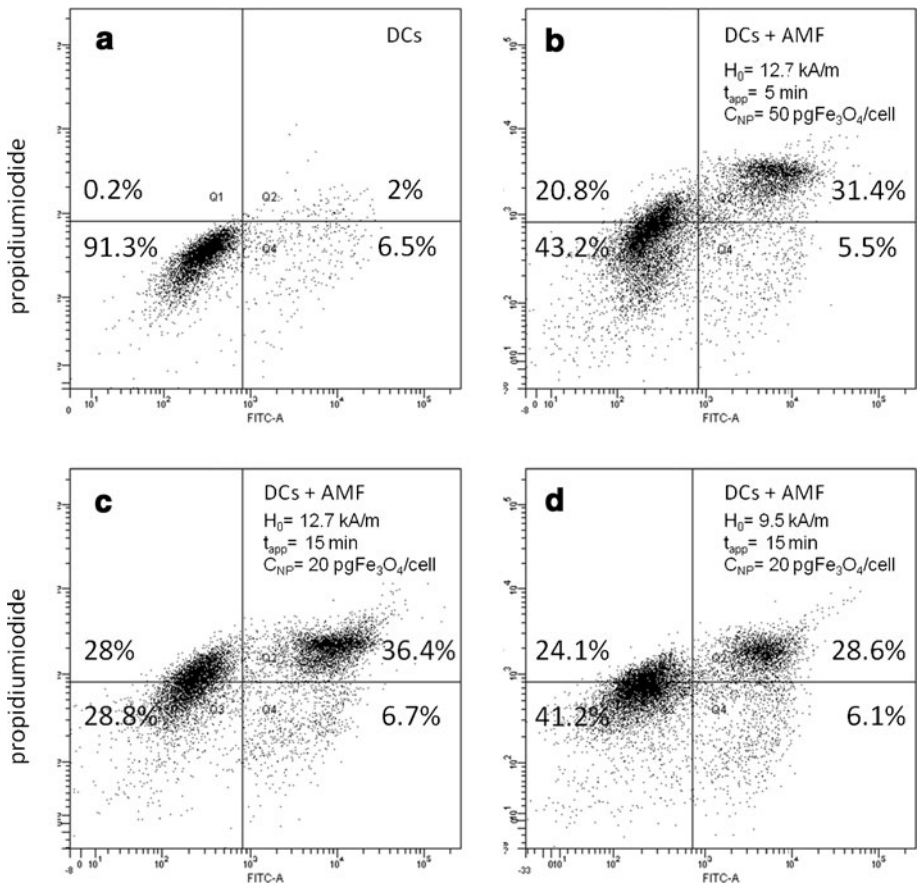

Fig. 9 Typical dot-plots obtained from FACS data showing DCs distribution (Annexin/Propidium Iodide (PI) staining) after exposure to different AMF amplitudes (H_0); exposure times (t_{app}) and incubation MNPs concentrations (C_{NP}). (**a**) Control DCs samples, showing 80–90% Annexin/PI dual negative population; (**b**) the shift in DCs population along the vertical axis after AMF exposure due to Annexin-negative/PI-positive cells; (**c**) and (**d**) dot plots representative of two independent experiments with different AMF amplitude and application times showing similar vertical shifts.

membrane integrity (26). In the present work, the amounts of MNPs incorporated into the DCs are below the required to increase the intracellular temperature during AMF exposure (see Fig. S3 in Supplementary Material and ref. (9)), and thus cell death is likely to be originated by intracellular mechanisms.

It has been reported that agglomeration of MNPs inside vesicles results in noticeable effects on their heating properties, i.e. to decrease their SPA due to increased magnetic dipolar-dipolar interactions (27). It is worth to mention that these results refer to the *average* temperature rise of the magnetic colloids as measured by a macroscopic temperature probe, which could differ from the local temperature inside the vesicles. The actual intracellular temperature at a given time will be the result of several factors such as the heat generation rate (i.e., the local power release) for a given experimental condition, and the thermal conductivity of the membranes and surrounding medium.

Although the systematic effects of application time t_{app} and MNPs concentration C_{NP} on cell viability are clear from Figs. 4 and 5, it can be noticed that there is a rather large dispersion of values for t_{app}=5 and 10 min, and C_{NP}= 20 pg(Fe_3O_4)/cell, i.e., the intermediate region of parameters at which cell death is triggered (see also Figures S1 and S2 of the Supplementary Material). This variability seems to be related to a) the nature of the DCs used, which are a primary cell culture and thus subjected to variations from sample to sample, and b) the nature of the triggering mechanisms involved in cell death. The primary nature of the DCs influences the reproducibility along different experimental runs (performed weeks apart from different buffy coats) but, since is also reflected in the control samples, can be taken into account. Regarding the effect of the triggering mechanism during AMF exposure, the observed dispersion of the results seems to be related to the existence of an energy threshold for breaking the endosomal compartments. Differences among individual cells should result in different amounts of uploaded MNPs within cells (and endosomes), and thus different energy thresholds for triggering cell death. This physical situation could explain the high sensitivity of the final result to experimental parameters.

The analysis of DCs viability from FACS data using Annexin V- Propidium Iodide (PI) markers suggests a necrotic-like process induced by AMF exposure. As can be seen from Fig. 9, a rather unique characteristic of the cell populations studied after AMF exposure is that the induced primary necrotic cells show Annexin V-negative/PI-positive staining (see also Figure S4 in the Supplementary Material). Fast membrane damage after few minutes of AMF exposure is consistent with a DCs population in which the affected cells show Annexin V-negative/PI positive staining before they become Annexin V-positive. We suggest that the cell death observed in DCs may be related to the degree of confinement of the MNPs found inside endosomal structures. These MNPs-agglomerates could be able to disrupt the endosomic membrane by the energy release during AMF application. Due to this membrane disruption, the release of the endosomal content into the cytoplasm is likely to damage the cell membrane, as reflected in the PI-positive DCs population. Although the precise pathways are not yet clear, the above results showed that it can provoke cell death after few minutes of AMF exposure on those previously MNPs-loaded DCs. Although this effect could only be valid for specific cell types, depending on the uptake of MNPs and their final intracellular distribution, targeting MNPs into a number of potentially relevant cell types could open the possibility of new therapeutic approaches.

CONCLUSIONS

We have demonstrated that is possible to control the amount of induced cell death of MNP-loaded dendritic cells, by adequate tuning of the physical AMF parameters and/or the final amount of MNPs in the intracellular medium. DCs cultures containing between 0.5 and 8 pg of Fe_3O_4 per cell showed a clear decrease of viable cells after AMF application times longer than 10 minutes. The observed decrease of viable cells should have a different origin from the 'usual' magnetic hyperthermia mechanism, since a negligible (2 to 4°C) temperature increase was observed during our experiments. Irrespective of the amount of viable cells after AMF application in different conditions, FACS analysis showed clear indication of a necrotic-like process on the cell population affected by the AMF. These data indicate that power release by the MNPs can locally alter relevant cell structures and/or metabolic processes yielding irreversible cell damage.

ACKNOWLEDGMENTS & DISCLOSURES

This work was supported by the Spanish Ministerio de Ciencia e Innovación (project MICINN MAT2010-19326 and CONSOLIDER NANOBIOMED CS-27 2006) and IBERCAJA. LA acknowledges MICINN by financial support through a FPU fellowship. The University of Zaragoza, along with their researchers, have filled patents related to the technology and intellectual property reported here. G.F. G. and M.R. I. have equity in nB Nanoscale Biomagnetics S.L. The other authors declare that they do not have any affiliations that would lead to conflict of interest. We are grateful to the I+CS staff (University Hospital, Zaragoza) Dr. J. Godino (FACS experiments) and Dr. M. Royo Cañas (confocal microscopy) for their advice and technical support.

REFERENCES

1. Woodhall B, Pickrell KL, Georgiade NG, Mahaley MS, Dukes HT. Effect of hyperthermia upon cancer chemotherapy - Application to external cancers of head and face structures. Ann Surg. 1960;151:750–9.
2. Turnbull AR. Hyperthermia and cancer. Lancet. 1975;1:643–4.
3. de Bree E, Theodoropoulos PA, Rosing H, Michalakis J, Romanos J, Beijnen JH, *et al.* Treatment of ovarian cancer using intraperitoneal chemotherapy with taxanes: From laboratory bench to bedside. Cancer Treat Rev. 2006;32:471–82.
4. Storm FK, Elliott RS, Harrison WH, Morton DL. Clinical rf hyperthermia by magnetic-loop induction - A new approach to human cancer-therapy. IEEE Trans Microw Theory Tech. 1982;30:1149–57.
5. Jordan A, Wust P, Fahling H, John W, Hinz A, Felix R. Inductive heating of ferrimagnetic particles and magnetic fluids - Physical evaluation of their potential for Hyperthermia. Int J Hyperthermia. 1993;9:51–68.
6. Magforce. "Magforce nanotechnologies ag receives european regulatory approval for its Nanocancer® therapy." 2010.
7. Matsuda H, Tsutsui S, Morita M, Baba K, Kitamura K, Kuwano H, *et al.* Hyperthermo-chemo-radiotherapy as a definitive treatment for patients with early esophageal-carcinoma. Am J Clin Oncol-Cancer Clin Trials. 1992;15:509–14.
8. Nie SM. Understanding and overcoming major barriers in cancer nanomedicine. Nanomedicine. 2010;5:523–8.
9. Marcos-Campos I, Asin L, Torres TE, Marquina C, Tres A, Ibarra MR, *et al.* Cell death induced by the application of alternating magnetic fields to nanoparticle-loaded dendritic cells. Nanotechnology. 2011;22:13.
10. Banchereauand J, Steinman RM. Dendritic cells and the control of immunity. Nature. 1998;392:245–52.
11. Guermonprez P, Valladeau J, Zitvogel L, Thery C, Amigorena S. Antigen presentation and T cell stimulation by dendritic cells. Annu Rev Immunol. 2002;20:621–67.
12. Trombettaand ES, Mellman I. Cell biology of antigen processing *in vitro* and *in vivo*. Annu Rev Immunol. 2005;23:975–1028.
13. Bodey B, Siegel SE, Kaiser HE. Antigen presentation by dendritic cells and their significance in antineoplastic immunotherapy. In Vivo. 2004;18:81–100.
14. Biragyn A, Ruffini PA, Leifer CA, Klyushnenkova E, Shakhov A, Chertov O, *et al.* Toll-like receptor 4-dependent activation of dendritic cells by beta-defensin 2. Science. 2002;298:1025–9.
15. Andersson LIM, Hellman P, Eriksson H. Receptor-mediated endocytosis of particles by peripheral dendritic cells. Hum Immunol. 2008;69:625–33.
16. Molavi L, Mahmud A, Hamdy S, Hung RW, Lai R, Samuel J, *et al.* Development of a Poly(D, L-lactic-co-glycolic acid) Nanoparticle Formulation of STAT3 Inhibitor JSI-124: Implication for Cancer Immunotherapy. Mol Pharm. 2010;7:364–74.
17. Basic specifications from the provider includes: Hydrodynamic size: 250 nm; NP concentration:10 mg/ml (4.9x1011 MNPs/ml); Polydispersity index < 0.2; MS (H = 1 T) = 67 emu/g., 2009.
18. Martin-Saavedra FM, Ruiz-Hernandez E, Bore A, Arcos D, Vallet-Regi M, Vilaboa N. Magnetic mesoporous silica spheres for hyperthermia therapy. Acta Biomaterialia. 2010;6:4522–4531.
19. Fortin JP, Gazeau F, Wilhelm C. Intracellular heating of living cells through Neel relaxation of magnetic nanoparticles. Eur Biophys J Biophys Lett. 2008;37:223–8.
20. Rodriguez-Luccioni HL, Latorre-Esteves M, Mendez-Vega J, Soto O, Rodriguez AR, Rinaldi C, *et al.* Enhanced reduction in cell viability by hyperthermia induced by magnetic nanoparticles. Int J Nanomed. 2011;6:373–380.
21. Duguet E, Hardel L, Vasseur S. Cell targeting and magnetically induced hyperthermia. Thermal nanosystems and nanomaterials, vol. 118. Berlin: Springer-Verlag Berlin; 2009. p. 343–65.
22. Prasad NK, Rathinasamy K, Panda D, Bahadur D. Mechanism of cell death induced by magnetic hyperthermia with nanoparticles of gamma-MnxFe2-xO3 synthesized by a single step process. J Mater Chem. 2007;17:5042–51.
23. Rabin Y. Is intracellular hyperthermia superior to extracellular hyperthermia in the thermal sense? Int J Hyperthermia. 2002;18:194–202.
24. Villanueva A, de la Presa P, Alonso JM, Rueda T, Martinez A, Crespo P, *et al.* Hyperthermia HeLa Cell Treatment with Silica-Coated Manganese Oxide Nanoparticles. J Phys Chem C. 2010;114:1976–81.
25. Creixell M, Bohorquez AC, Torres-Lugo M, Rinaldi C. EGFR-targeted magnetic nanoparticle heaters kill cancer cells without a perceptible temperature rise. ACS Nano. 2011;5:7124–7129.
26. Lunov O, Zablotskii V, Pastor JM, Perez-Landazabal JI, Gomez-Polo C, Syrovets T, *et al.* Thermal Destruction on the Nanoscale: Cell Membrane Hyperthermia with Functionalized Magnetic Nanoparticles. In: Hafeli U, Schutt W, Zborowski M, editors. 8th Internatioanl Conference on the Scientific and Clinical Applications of Magnetic Carriers, Vol. 1311, Amer Inst Physics, Melville, 2010, pp. 288–292.
27. Beaune G, Levy M, Neveu S, Gazeau F, Wilhelm C, Menager C. Different localizations of hydrophobic magnetic nanoparticles within vesicles trigger their efficiency as magnetic nano-heaters. Soft Matter. 2011;7:6248–54.